

# Optimization of Process Parameters for Automated Drilling with Unidirectional Clamping of Aerospace Aluminum Alloys

Weina Jing

*Engineering Technology Training Center, Civil Aviation University of China, Tianjin, China*

**Abstract:** As the primary load-bearing structure of aircraft, the reliability and safety of aluminum alloy structures' connections are paramount, making drilling techniques and processes crucial. This paper focuses on the unidirectional clamping drilling process, a key application technology, analyzing the impact of various process parameters on processing quality. The aim is to provide valuable insights for the engineering application of automated drilling technology for aerospace aluminum alloys.

**Keywords:** Aerospace Aluminum Alloys; Drilling Process; Burr; Clamping Force

## 1. Introduction

The assembly of aircraft components is a vital part of the aircraft manufacturing process, and the quality of the final aircraft heavily depends on the successful assembly of these intricate components [1]. Therefore, to achieve high-quality, long-lasting, cost-effective, and efficient assembly connections that meet the development requirements of aircraft structures, significant efforts are necessary [2]. Aluminum alloys occupy a significant proportion of aircraft structural materials, and researching drilling processes for aluminum alloys is of great significance to achieving perfect alignment in the component assembly process.

Automated drilling technology is a core technology in aerospace manufacturing, encompassing critical aspects such as flexible tooling technology, measurement technology, and inspection technology. The process of automated drilling also plays a pivotal role in processing quality [3]. Consequently, this paper delves into some of the key process issues in automated drilling of aerospace aluminum alloys, aiming to provide valuable references for the engineering application of automated drilling technology for aerospace aluminum alloys.

## 2. Construction of Unidirectional Clamping

### Drilling Model

During drilling operations, burrs are not only formed at the drill exit but also between the layers of the processed materials, known as interlayer burrs. In the automated assembly process of aircraft, holes are often drilled in stacked layers of aerospace materials, requiring consistent assembly continuity. Traditional drilling methods involve disassembling parts after drilling to remove burrs, significantly impacting assembly efficiency and automation [4-5]. Therefore, adopting methods to control and reduce interlayer burrs can eliminate the need for interlayer burr removal or even secondary clamping, significantly enhancing the efficiency of automated drilling processes. This approach falls under the category of active burr control technology [6-7].

Applying localized clamping force during the drilling process to "integrate" the assembled parts during hole-making can control the growth of interlayer burrs, limiting their size to a minimal range. Thus, the application of clamping force is an effective active burr control technique [8-9].

Different automated drilling equipment utilizes distinct clamping methods [10]. One is unilateral clamping, and the other is bilateral clamping, as illustrated in Figure 1. Automated drilling equipment used in aircraft assembly, such as crawling robots and automatic riveting machines, are typically located outside the panel and adopt unilateral clamping [11]. Industrial robot automatic drilling systems, which can add robots on the back of the panel for dual-robot collaborative drilling, can utilize bilateral clamping [12]. To simulate the clamping force in automated drilling, two cylinders are used to provide the clamping force. The experimental clamping device is shown in the figure. As depicted in Figure 2, a ring gasket is fixed to the upper plate connected to the cylinders, simulating a pressure foot. During drilling, the gasket applies pressure around the hole, and the clamping force is applied by the cylinders. The

air pressure in the cylinders is adjusted using a pressure regulating valve to obtain different

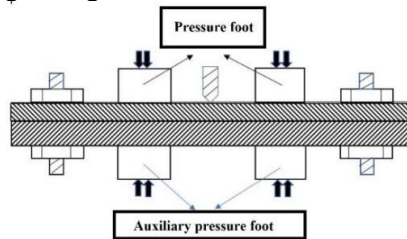
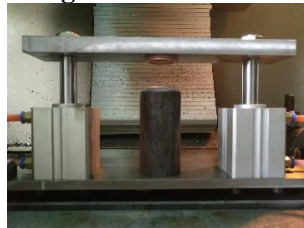
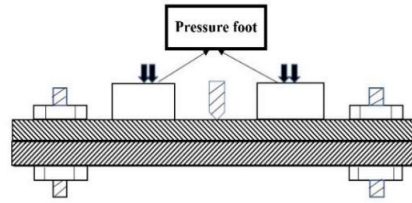


**Figure 1. Geometric Models of Unilateral and Bilateral Clamping**



(a) Clamping Device



(b) Bilateral Clamping Effect

**Figure 2. Clamping Device**

### 3. Optimization of Drilling Process Parameters

#### 3.1 Experimental Equipment

##### 3.1.1 Experimental Materials

The drilling experiments employ 2024-T3 aviation aluminum alloy, which primarily comprises Cu, Mg, Mn, with impurities such as Fe and Si. This alloy exhibits high plasticity, fatigue life, fracture toughness, resistance to fatigue crack propagation, heat resistance, and yield strength. Thick plates of this alloy are primarily used in aircraft fuselages, wings, shear ribs, webs, and other structural components requiring high strength.

##### 3.1.2 Cutting Tools and Equipment

The cutting tool is a WALTER solid carbide straight-shank drill, model A3367-4, with a diameter of 4mm. The processing equipment is a DMG Mori three-axis vertical machining center, model DMC 635V eco, equipped with a Siemens 810D CNC system.

##### 3.1.3 Testing Equipment

A universal 3D coordinate video measuring machine, also known as an optical video measuring instrument, is shown in Figure 3. Its technical parameters are shown in Table 1.

**Table 1. ZIP250 3D Coordinate Video Measuring Machine Technical Parameters**

Technical Parameter Indicator	Value
X/Y/Z Axis Measurement Stroke (mm)	250*150*200
X/Y Axis Linear Accuracy ( $\mu\text{m}$ )	X/Y:E2=1.8+4L/1000um Z:E1=2.5+5L/1000um

clamping forces.

Z Axis Linear Accuracy ( $\mu\text{m}$ )	30-170 x
--	----------



**Figure 3. 3D Coordinate Video Measuring Machine**

#### 3.2 Experimental Plan

According to the mechanism of burr formation, the axial drilling force causes plastic deformation in the workpiece, which is the most critical factor influencing burr generation. When the workpiece material and cutting tool are fixed, the axial force is only related to the feed rate. Therefore, the entire drilling process is divided into four zones: the feed-in zone, cutting zone, feed-out zone, and retraction zone, as shown in Figure 4.

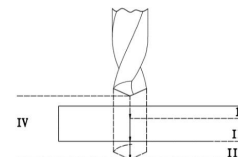


**Figure 4. Processing Area**

Under these four zones, we employ two different processes: single-pass feed and multi-layer feed. The single-pass feed involves maintaining a consistent feed rate across all four zones at a specific rotational speed. The multi-layer feed, on the other hand, involves varying the feed

rates in the four zones at a specific rotational speed, as outlined in Table 2.

The single-pass feed process involves using the same feed rate throughout the entire feed process. In contrast, the multi-layer feed process divides the four zones into specific distances, and at rotational speeds of 5000/7000/11000 (r/min), the feed rate changes according to the

predefined scheme. For example, at Speed Number 1, the feed rate starts at 50 mm/min in the feed-in zone, increases to 100 mm/min upon entering the cutting zone (after 0.5mm), decreases to 100 mm/min in the feed-out zone (after 1.5mm), and finally increases to 500 mm/min in the retraction zone (after 2mm), completing the entire process in this manner

**Table 2. Specific Process Plans for Single-Pass Feed and Multi-Layer Feed**

Scheme	Scheme Process Parameters					
	Rotation Speed n/(r/min)	Feed Rate F (mm/min)				
		Feed Rate Number	Feed-in Area	Cutting Area	Feed-out Area	Retraction Area
Scheme1 Single Feed	5000/7000/11000	100/300/500/700/900/1100/1300/1500 (Same parameters for all areas)				
Scheme 2 Segmented Feed Feed-in Area 0.5mm Cutting Area 1.5mm Feed-out Area 2mm Retraction Area 6mm	5000/ 7000/ 11000	1	50	100	100	500
		2	100	300	200	500
		3	150	500	300	500
		4	200	700	400	500
		5	250	900	500	500
		6	300	1100	600	500
		7	350	1300	700	500
		8	400	1500	800	500

### 3.3 Analysis of Experimental Results

#### 3.3.1 Influence of Process Parameters on Hole Diameter Accuracy

Using the optical video measuring machine, we tested the diameter of the holes and recorded the data. Based on these data, we compared and analyzed the hole diameters under different feed methods and rotational speeds of 5000/7000/11000 (r/min), as presented in Tables 3-5.

From the experimental data, it can be observed that the hole diameter accuracy is generally good, and there is no apparent regularity in the influence of different process parameters on hole diameter accuracy.

**Table 3. Hole Diameters at 5000 r/min with Different Processes**

Single-Pass Feed		Multi-Layer Feed	
Feed Rate mm/min	Hole Diameter mm	Feed Rate Number	Hole Diameter mm
100	4.08160	1	4.08938
300	4.06085	2	4.08100
500	4.05908	3	4.08300
700	4.08173	4	4.07940
900	4.08452	5	4.08708
1100	4.10775	6	4.09658
1300	4.08200	7	4.09216
1500	4.09558	8	4.10308

**Table 4. Hole Diameters at 7000 r/min with Different Processes**

Single-Pass Feed		Multi-Layer Feed	
Feed Rate mm/min	Hole Diameter mm	Feed Rate Number	Hole Diameter mm
100	4.07932	1	4.08002
300	4.10260	2	4.05225
500	4.12413	3	4.05732
700	4.06578	4	4.08918
900	4.12458	5	4.10852
1100	4.08728	6	4.11930
1300	4.05935	7	4.16588
1500	4.08270	8	4.13870

**Table 5. Hole Diameters at 11000 r/min with Different Processes**

Single-Pass Feed		Multi-Layer Feed	
Feed Rate mm/min	Hole Diameter mm	Feed Rate mm/min	Hole Diameter mm
100	4.06496	1	4.09312
300	4.04308	2	4.091175
500	4.06100	3	4.06052
700	4.66468	4	4.05735
900	4.07532	5	4.07706
1100	4.08263	6	4.06835
1300	4.06402	7	4.06116
1500	4.07098	8	4.08161

### 3.3.2 Influence of Process Parameters on Scratch Width

After hole drilling, we utilized an optical image measuring instrument to measure the scratch width of each hole. The measurement diagram is shown in Figure 5, and the scratch width data are shown in Tables 6-7.

According to the experimental data, the ORIGIN curve graph of scratch width under different processes at the rotational speeds of 5000/7000/11000 (r/min) is drawn as shown in Figure 6.

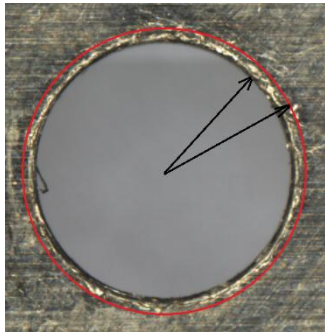


**Figure 5. Schematic Diagram of Scratch Width**

**Table 6. Relationship Between Rotation Speed and Scratch Width under Single-Feed Process.**

Feed Rate mm/min	Rotation Speed r/min		
	5000	7000	11000
100	0.05780	0.06730	0.00900
300	0.09950	0.08595	0.99250
500	0.10960	0.09370	0.08776
700	0.13825	0.11843	0.15025
900	0.15440	0.13376	0.16320
1100	0.13825	0.15975	0.17150
1300	0.19600	0.17848	0.19160
1500	0.19000	0.17373	0.19200

**Table 7. Relationship Between Rotation Speed and Scratch Width under Multi-Feed Process**

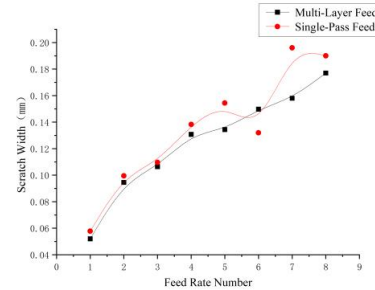
Feed Rate Number	Rotation Speed r/min		
	5000	7000	11000
1	0.05200	0.06424	0.07100
2	0.09450	0.08390	0.096750
3	0.10640	0.09310	0.08900
4	0.13075	0.10318	0.14950
5	0.13440	0.12880	0.16500
6	0.14575	0.15548	0.16525
7	0.15800	0.16944	0.17780
8	0.17700	0.17223	0.18750

Observations from Figure 6:

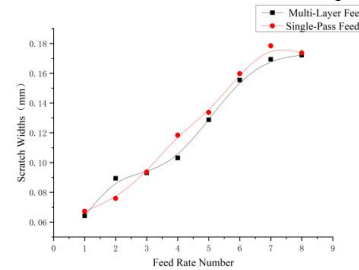
1. The scratch width increases with the increase in feed rate.

2. The scratch width is generally controlled within 0.2mm.

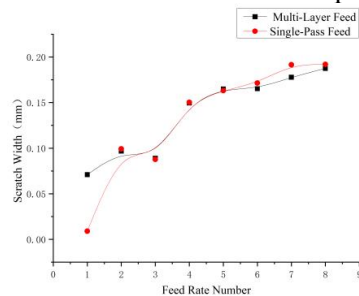
3. At the same feed rate, the scratch width of the multi-layered feed process is smaller than that of the single-feed process.



**(a) ORIGIN Curve of Scratch Widths under Different Processes at 5000 rpm**



**(b) ORIGIN Curve of Scratch Widths under Different Processes at 7000 rpm**



**(c) ORIGIN Curve of Scratch Widths under Different Processes at 11000 rpm**

**Figure 6. ORIGIN Curves of Scratch Widths under Different Processes at Different Rotation Speeds**

### 3.3.3 Influence of Process Parameters on Burr Height

The burr morphology of holes obtained using different process parameters can be classified into three main types: uniform burrs, burrs with a drill cap, and uneven coronal burrs, as shown in Figure 7.

The formation processes of these three types of burrs are analyzed based on their mechanisms as follows:

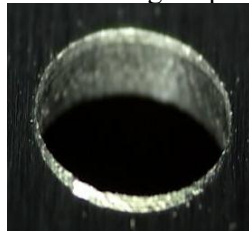
(1) Uniform Burrs: They fully comply with the five steps of burr growth. Initially, the drill performs normal cutting, during which a large amount of chips are cut off by the main cutting

edge and expelled along the helical flute (rake face), with the machining taking place entirely within the workpiece. The secondary cutting edge repeatedly cuts, resulting in no burrs on the inner wall of the hole. As drilling progresses, when the hole is about to be drilled through, the material at the bottom of the workpiece undergoes significant plastic deformation under the action of the drill, and is subsequently pushed out, initiating the formation and development of burrs. Further drilling intensifies the plastic deformation until the end material fractures, ultimately leaving some chips uncut by the drill, forming a uniformly distributed burr around the hole exit.

(2) Burrs with a Drill Cap: These burrs, commonly formed at lower feed rates and drilling speeds, occur when the material at the workpiece bottom undergoes plastic deformation

under the influence of the chisel edge as the drill nears breakthrough. The plastic deformation spreads from the chisel edge to the surrounding area, continues to deform until it cracks, and partially detaches from the workpiece, forming a drill cap.

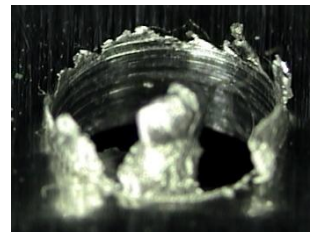
(3) Uneven Coronal Burrs: These burrs exhibit uneven height distributions and are generally larger in size, affecting machining accuracy and being difficult to remove. They typically form under high feed rates and low drilling speeds. A high feed rate leads to a large drilling force, causing significant plastic deformation of the material. As drilling nears completion, the material at the hole exit experiences high compressive stress, leading to fracture in the central region and extrusion-tension of surrounding material, resulting in uneven coronal burrs.



(a) Uniform Burrs



(b) Burrs with a Drill Cap



(c) Uneven Coronal Burrs

**Figure 7. Burr Morphology**

Tables 8-9 show the data obtained after measuring the burr height with the optical image measuring instrument.

The ORIGIN curve graph of burr height of holes obtained by different processes at various rotational speeds is drawn as shown in Figure 8.

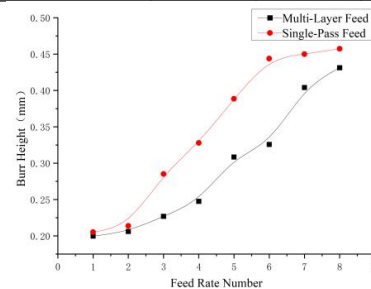
**Table 8. Burr Heights under Single-Process (mm)**

Feed Rate mm/min	Rotation Speed r/min		
	5000	7000	11000
100	0.20520	0.19560	0.19220
300	0.21375	0.20700	0.202250
500	0.28520	0.27460	0.26400
700	0.32775	0.33175	0.35272
900	0.38860	0.37300	0.33340
1100	0.44400	0.43125	0.42050
1300	0.45000	0.44780	0.43000
1500	0.45750	0.45325	0.44475

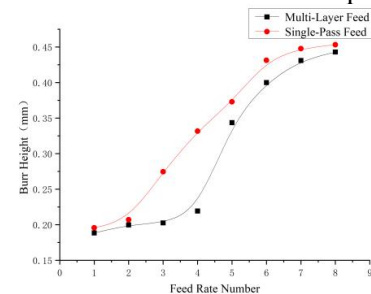
**Table 9. Burr Heights under Multi-Process (mm)**

Feed Rate Number	Rotation Speed r/min		
	5000	7000	11000
1	0.19960	0.18840	0.18000
2	0.20600	0.19975	0.193750
3	0.27680	0.20260	0.19600

4	0.31750	0.21925	0.21025
5	0.37840	0.34360	0.33080
6	0.43575	0.40000	0.39175
7	0.44060	0.43100	0.42220
8	0.45125	0.44300	0.43200

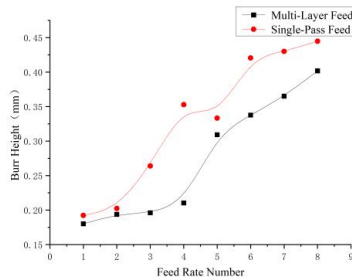


(a) ORIGIN Curve of Burr Heights under Different Processes at 5000 rpm



(b) ORIGIN Curve of Burr Heights under Different Processes at 7000 rpm





(c) ORIGIN Curve of Burr Heights under Different Processes at 11000 rpm

**Figure 8. ORIGIN Curves of Burr Heights under Different Processes at Different Rotation Speeds**

Observations: At the same rotation speed, burr height increases with the increase in feed rate. Under the same process parameters, the burr height of the multi-layered feed process is lower than that of the single-feed process.

#### 4. Conclusion

The influence of processing parameters on the quality of hole machining: As the feed rate increases, the scratch width generally exhibits an increasing trend. The scratch width at the hole entrance under both single-pass and multi-layer feed processes can basically be controlled within 0.2mm; the scratch width of the multi-layer feed process is slightly smaller than that of the single-pass process. When the rotation speed remains constant, the burr height increases with the increase of the feed speed; compared with the single-pass process, the multi-layer feed process can effectively suppress burr formation and control burr growth.

#### Acknowledgments

Supported by the Fundamental Research Funds for the Central Universities, NO. 3122015D006 (Research on High-quality Processing Technology of Fastening Holes in Aircraft)

#### Reference

- [1] Wang Wenli, Shao Kun, Luo Rui, Yan Wei, Chang Chang. High-Speed Milling Process of Aircraft Large-Scale Aluminium Alloy Integral Wall Panel [J]. Aeronautical Manufacturing Technology, 2022,65(15):82-86.
- [2] Chen Shuai, Liu Xule, Chen Lei. A Compact End Effector for Aircraft Assembly Drilling[J]. Modern Manufacturing Technology and Equipment, 2023,59(4):80-82.
- [3] Wang Wei, Wang Min, Chen Wenliang, Xu Qinghe, Huang Wen, Jiang Hongyu. Optimization of pressing force considering instantaneous springback in skin-side pressed drilling[J]. Journal of Beijing University of Aeronautics and Astronautics. 2020,46(01):210-219.
- [4] Liu Xuefeng, Zhu Weidong, Yang Guorong, Dang Xiaojuan. Clamping force prediction for automatic drilling of stacked thin-walled workpieces based on finite element method[J]. Journal of Central South University (Science and Technology) 2018,49(02):339-344.
- [5] Zhang Xinming, Liu Shengdan. Aircraft Aluminum Alloys and Their Materials Processing [J] Materials China. 2013,32(1):40-46.
- [6] Jiang Liping, Chen Wenliang, Wang Min, Liu Yuling, Hou Yuzhao. An Approach to Adaptive Response Surface Optimization of One-side Pressed Drilling Process [J]. China Mechanical Engineering, 2015,26(23).
- [7] Yuan Hongxuan. Manufacturing Technology of Connecting Hole in Aircraft Structures[J]. Aeronautical Manufacturing Technology, 2007, 18(1):97-99.
- [8] Liu Bing, Peng Chao-qun, Wang Ri-chu, Wang Xiao-feng, Li Ting-ting. Recent development and prospects for giant plane aluminum alloys[J] The Chinese Journal of Nonferrous Metals, 2010,20(9):1706-1712.
- [9] Hong Huazhou, Wei Hongyu, Chen Wenliang, Jin Xia, Jiang Hongyu, Wang Yubo, Yu Lu. Control Process for Drilling Burr Growth of Aerospace Thin-walled Workpiece[J]. China Mechanical Engineering, 2012,23(19):2312-2315.
- [10] Lu Zhijun. Study of One-Side Pressed Drilling Process of Aluminum Alloy Thin-Walled Laminated Structure[J] Aeronautical Manufacturing Technology. 2015,(S2):152-156.
- [11] Liu Zi. Research on precision hole making process for laminated materials of aircraft panel[D]. Nanjing University of Aeronautics and Astronautics College of Mechanical and Electrical Engineering 2015
- [12] Wang Wei. Research on One-side Pressed Automatic Drilling Process with Multi-parameter Combined Action[D]. Nanjing University of Aeronautics and Astronautics College of Mechanical and Electrical Engineering 2020.